FINAL TECHNICAL REPORT

Intraslab Seismicity and Seismic Structure of the Northern Cascadia Subduction Zone

Award Number: 02HQGR0045

Principal Investigators: Michael G. Bostock & Todd A. Nicholson

Department of Earth and Ocean Sciences, The University of British Columbia
6339 Stores Road, Vancouver, B.C., Canada, V6T 1Z4
Tel: 604-822-2082; Fax 604-822-6088; email: bostock@eos.ubc.ca

NEHRP Element III (PN)

Research supported by the U.S. Geological Survey (USGS), Department of the Interior, under USGS award number 02HQGR0045). The views and conclusions contained in this document are those of the authors and should not be interpreted as necessarily representing the official policies, either expressed or implied, of the U.S. Government.

02HQGR0045

INTRASLAB SEISMICITY AND SEISMIC STRUCTURE OF THE NORTHERN CASCADIA SUBDUCTION ZONE

Michael G. Bostock and Todd A. Nicholson
Department of Earth and Ocean Sciences
The University of British Columbia
6339 Stores Road, Vancouver, B.C.
Canada V6T 1Z4
Tel: 604-822-2082; Fax: 604-822-6088; email: bostock@eos.ubc.ca

TECHNICAL ABSTRACT

A detailed passive seismic experiment was carried out across southwestern British Columbia and northwestern Washington to investigate the structure of the subducting Juan de Fuca plate and mantle wedge in Cascadia and its relation to intra-slab seismicity. A total of 31 three component, broadband stations were deployed in an approximately linear array, spanning southern Vancouver Island, the Gulf and San Juan Islands, Watcom county and the British Columbia lower mainland. P-wave coda from 41 teleseismic events have been employed in formal inversions for fine-scale shear-velocity structure. Our results indicate a structure very similar to that identified across a comparable profile in central Oregon. The continental Moho is evident at the eastern end of the profile near 35 km depth but disappears towards the Georgia Strait/Puget Sound. A prominent low S-velocity zone is clearly evident below southern Vancouver Island dipping eastward through Georgia Strait/Puget Sound and coincides with the E-reflection zone originally identified in LITHOPROBE studies. Structure below the E-layer is much less prominent and varies intermittently along the array. Based on the observations and interpretations of similar structures beneath Oregon, Alaska and South America, and its projection to mantle depths, we suggest that the low-velocity E-layer represents the dehydrating oceanic crust of the subducting Juan de Fuca plate. This interpretation is consistent with recent seismicity studies, that place shallow Wadati-Benioff events within the oceanic mantle, and implies that the oceanic crust is 6-8 km shallower beneath Vancouver Island than previously assumed. As in Oregon, we interpret the diminished signature of oceanic crust below a depth of 45 km to signal the presence of eclogitization, which in turn supplies water to serpentinize the overlying forearc mantle.

NON-TECHNICAL ABSTRACT

An array of seismometers was deployed across southern Vancouver Island, the Gulf and San Juan Islands, Watcom county, and the greater Vancouver region to examine the relation between deep earthquakes and the structure of the downgoing Juan de Fuca (oceanic) plate as it subducts below the northern Washington and southern British Columbia. Our results clearly reveal a 10 km thick, seismic low-velocity layer, 20 km below the west coast of Vancouver Island that dips northeastward below the Georgia Strait/Puget Sound to depths of more than 50 km. We outline additional evidence from similar studies in central Oregon and elsewhere, slab earthquake locations, and reflection seismology that supports an interpretation that this low-velocity layer is the topmost portion (*i.e.* oceanic crust) of the downgoing plate. This interpretation places the main Cascadia thrust fault, separating the Juan de Fuca and North American plates, between 5 and 10 km more shallow than previously thought, a result with important consequences for our understanding of slab earthquakes and plate dynamics in this region.

1 Introduction

The Cascadia subduction zone dominates the tectonic setting along the western coast of North America from southern British Columbia to northern California. In this region, the Juan de Fuca plate system subducts beneath the much larger North American plate. In the past 20 years, numerous studies have demonstrated the complexity of upper mantle structure beneath southern Vancouver island in northern Cascadia, *e.g.Green et al.*, 1986; *Kurtz et al.*, 1986; *Cassidy & Ellis*, 1991; *Clowes & Hyndman*, 2002; *Nedimovic et al.*, 2003; *Calvert et al.*, 2003]. This complexity has led to several competing interpretations of both major structural features [*e.g.*, *Clowes & Hyndman*, 2002; *Nedimovic et al.*, 2003] and finer details of the subduction complex [*e.g.*, *Green et al.*, 1986; *Clowes et al.*, 1987; *Calvert & Clowes*, 1990; *Calvert et al.*, 2003]. In particular, considerable controversy centres on the position of the subducting oceanic crust, the so-called E-reflectors (a group of strong seismic reflectors), and the precise roles these two features play in the subduction process. Needless to say, the location of the plate boundary is a first order issue that must be resolved before the prevailing geodynamic processes [*e.g.*, [*Dragert et al.*, 2001; *Hyndman & Wang*, 2003; *Rogers & Dragert*, 2003] can be fully understood.

Previous geophysical studies have utilised seismic reflection [*e.g.*, *Yorath et al.*, 1985; *Green et al.*, 1986], seismic refraction [*e.g.Clowes et al.*, 1995], traveltime tomography [*e.g. Ramachandran*, 2001], magnetotellurics [*Kurtz et al.*, 1986], and seismicity [*Cassidy & Waldhauser*, 2003] to construct profiles of subsurface physical properties (P-velocity, reflectivity, conductivity, hypocentre distribution) across southern Vancouver Island. In addition, *Cassidy and Ellis* [1991] and *Cassidy* [1995] have produced local estimates of geometry and material properties of dipping layers beneath central Vancouver Island at a number of broadband seismic stations using receiver function analysis. This latter approach employs scattered waves in the teleseismic P-coda caused by conversions and/or reflections at subsurface interfaces that are particularly useful due to their sensitivity to S-velocity variations and because both the magnitude and, perhaps more importantly, the polarity of subsurface velocity contrasts can be reliably determined.

In this study we extend the work of *Cassidy & Ellis*, [1991] and *Cassidy* [1995] by examining a new multichannel teleseismic dataset across southern Vancouver Island and adjacent Washington and southern British Columbia. This dataset provides a more spatially continuous sampling than these previous receiver function studies allowing for direct comparison with other geophysical profiles. Moreover, results from a similar experimental configuration in Oregon [*Nabelek*, 1993; *Rondenay et al.*, 2001; *Bostock et al.*, 2002] have provided clear signatures of the subducting plate. We begin our analysis by demonstrating the sensitivity of teleseismic P coda to upper mantle structure in northern Cascadia. We then use the approach of *Frederiksen & Bostock* [2003] to constrain the orientation and material properties of prominent upper mantle structure by modelling the subduction zone as a series of dipping layers. This inversion also allows the material properties of the surrounding material to be constrained. The migration inversion approach of *Bostock et al.*, [2001] is then used to study deviations from this simple layered model and to investigate lithospheric structure in the forearc.

2 Tectonic Setting and Previous work

Convergence has dominated plate interaction along the western margin of North America for at least the past 150 million years [*Riddihough*, 1982; *Engebretson et al.*, 1992]. Off the coast of Oregon, Washington and southern Vancouver Island the relatively young (maximum age ~10 million years), warm Juan de Fuca plate subducts beneath the North American plate (see figure 1). Convergence is currently occurring at a rate of 40-47 mm/a directed Ndeg 56E-Ndeg 68E [*Riddihough & Hyndman*, 1991; *DeMets et al.*, 1990].

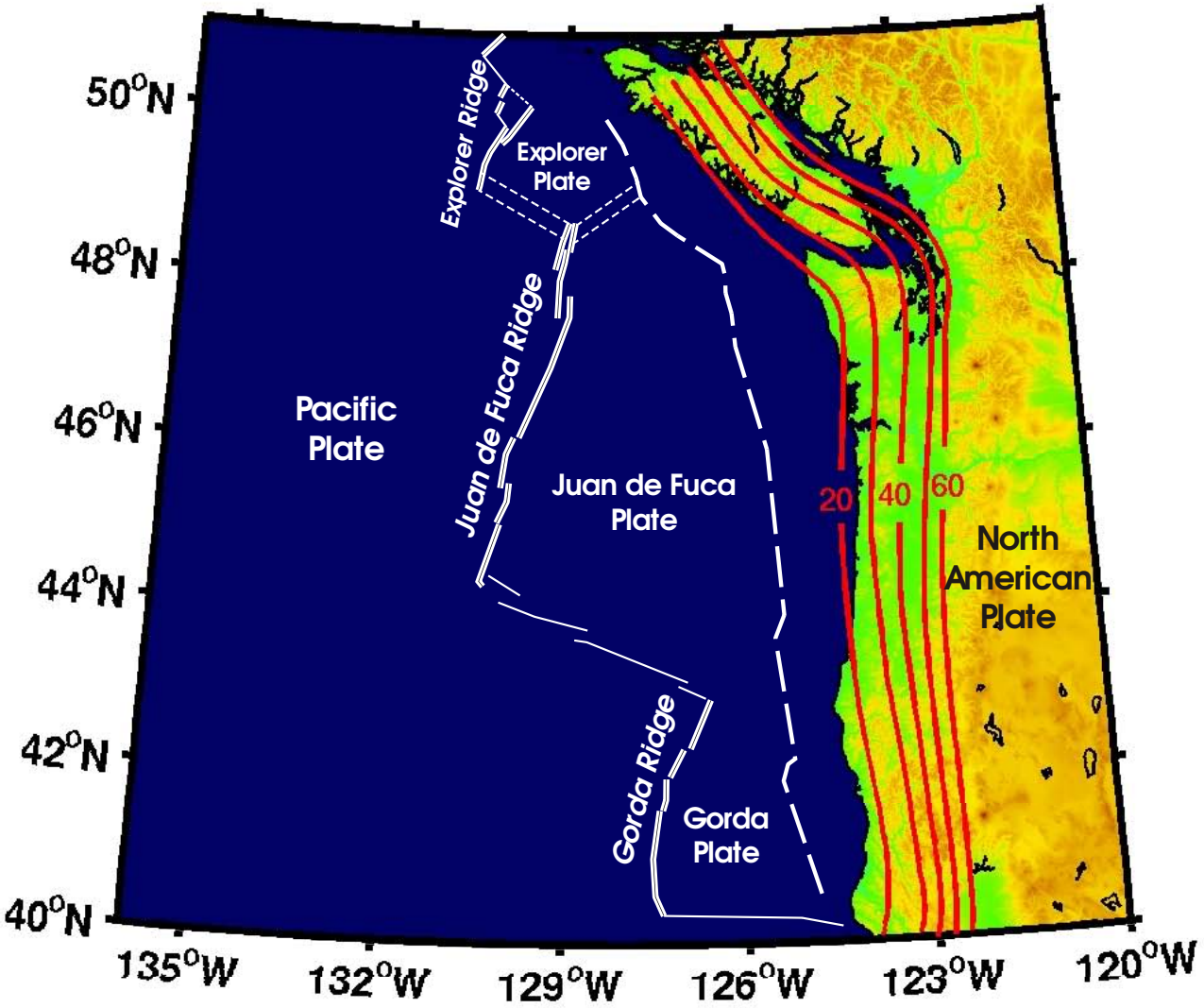

Figure 1: Map of the Cascadia subduction zone. The contours show the depth (labelled in km) of the top of the subducting crust (Wang pers. comm.).

Current understanding of subsurface structure beneath Vancouver Island and the Georgia Strait derives primarily from seismic reflection studies [see summary by *Clowes & Hyndman*, 2002]; in particular the LITHOPROBE and SHIPS programs. Much attention has been focused on the position of the subducted oceanic crust and a zone of unusually prominent seismic reflectors known as the E-reflectors (or E-layer). In the first studies of the 1984 LITHOPROBE

lines [*Green et al.*, 1986], the E-layer was interpreted as a layer at the top of the subducting oceanic lithosphere. In 1985, a series of marine reflection surveys were conducted west of Vancouver Island showing a clear reflection that can be unequivocally identified as the top of the Juan de Fuca plate [*Clowes et al.*, 1987; *Drew & Clowes*, 1990]. Although faint in some areas the top of the plate can be traced to the eastern edge of the profiles (∼20 km west of Vancouver Island) whereupon it becomes more difficult to distinguish. Beneath Vancouver Island the top of the plate is now commonly proposed to correlate with an intermittently imaged weak reflection known as the F-reflector on the LITHOPROBE lines [*e.g.*, [*Drew & Clowes*, 1990; *Calvert*, 2004]. This interpretation places a gap of 5-8 km between the bottom of the E-layer and the top of the oceanic crust and is loosely based on a combination of the offshore profiles, hypocentre data and receiver function analysis [*Cassidy & Ellis*, 1991; *Cassidy*, 1993]. The latter study identified the F reflector as the upper boundary of a weak low S-wave velocity zone, broadly consistent with the interpreted oceanic crust. A new interpretation was proposed by *Nedimovic et al.* [2003] who associated the top of the oceanic crust with the bottom of the E-reflectors, based on analysis of reflection data, seismicity and tomographic velocities. To complicate matters further, *Preston et al.* [2003] proposed that shallow-most (< 45 km) Benioff events in Cascadia, such as those beneath western Vancouver Island, may actually lie within the Juan de Fuca plate mantle (the result of serpentine dehydration) rather than within the subducted crust, as previously assumed. Consequently, seismicity constraints on the position of the plate may need to be reconsidered. The utility of seismicity in precisely locating the plate is also compromised by location errors, although approaches such as double differencing [*Waldhauser*, 2000]; arrival pattern location [*Nicholson et al.*, 2002] and 3-D empirical travel times [*Nicholson et al.*, 2004] have recently improved location accuracy. Resolution of the debate concerning the position of the subducted crust is of central importance in resolving important geodynamic questions [*Rogers & Dragert*, 2003].

Despite uncertainty surrounding the location of the downgoing plate, much has been learned about the geometry and character of the E-reflectors [*Clowes & Hyndman*, 2002]. The reflectors form a thin (< 2 km) zone off the coast of central Vancouver Island [*Calvert*, 1996; *Nedimovic et al.*, 2003] but thicken to 12-15 km off the coast of southern Vancouver Island [*Calvert et al.*, 2003] and appear to be 5 to 8 km thick inland of the western coast of Vancouver Island [*Green et al.*, 1986; *Nedimovic et al.*, 2003]. It is unclear at what depth the E-reflection zone terminates. *Nedimovic et al.* [2003] interpret the E-reflectors to end abruptly where the bottom of the zone encounters the forearc mantle, at a depth of 33±3 km. *Calvert et al.* [2003], on the other hand, demonstrate that the E-reflectors to persist to a depth of at least 50 km. Part of this disagreement could be explained by differences in transect position.

[*Kurtz et al.* [1986] used magnetotelluric data to show that the E-layer is highly conductive across most of Vancouver Island. The E-layer and C-layer (a second, weaker, shallower zone) are also thought to possess low density [*e.g.*, *Clowes et al.*, 1997] and low P-wave velocity [*Drew & Clowes*, 1990], although it should be noted that recent tomographic models do not clearly demonstrate this latter property [*Ramachandran*, 2001; *Preston et al.*, 2003]. Receiver function studies have shown that the C-layer is less prominent than the underlying E-layer and that both are low S-velocity zones. There have been several explanations proposed to explain the high reflectivity and low S-wave velocity of the E-layer as well as the observation that it extends to mantle depths. These include interpreting the E-layer as:

1. The top of the subducting Juan de Fuca plate [*Green et al.*, 1986], although this interpretation is now largely discounted.

2. Interlayered mafic and/or sedimentary rocks [*Yorath et al.*, 1985; *Clowes et al.*, 1987].

3. Intensely sheared sediments that trap fluids released from the subducting plate [*Calvert & Clowes*, 1990].

4. Thin dipping fluid filled lenses of high porosity, where fluid is supplied by dehydration reactions within the underlying oceanic plate [*Hyndman*, 1988].

It has also been proposed that the E-reflectors may represent a zone of ongoing deformation associated with the slow slip events observed along the Cascadia subduction zone [*e.g.*, *Nedimovic et al.*, 2003; *Calvert*, 2004] with a well defined 14 month periodicity.

3 Data and Processing

In the period April 2002 - November 2002, 26 broadband seismometers were deployed by the POLARIS consortium across the northern Cascadia subduction zone to supplement 5 permanent broadband stations operated by the Geological Survey of Canada (see figure 2). Together these 31 stations form the POLARIS-BC array - an approximately linear array spanning southern Vancouver Island, the Strait of Georgia, coastal Washington and the British Columbia Fraser Valley. The array will operate until December 2004.

As at January 2004, 40 teleseismic events of magnitude 6.0 or greater and with high signal-to-noise ratio had been recorded by the POLARIS-BC stations (see figure 3). Azimuthal coverage is relatively good since almost the entire Pacific, central and South America lie within the range of teleseismic P (deg 30-deg 100). The azimuthal coverage is poor only to the south and north-east of the study region.

Near-vertically propagating teleseismic P waves are scattered and reflected by near receiver structure in a variety of ways. Figure 4 shows the three most useful scattering modes for events up-dip and down-dip from a planar dipping structure. Receiver function analysis [*e.g.*, *Langston*, 1979; *Cassidy & Ellis*, 1991] focusses mainly on the forward-scattered P-s mode and the other two modes are frequently viewed as sources of noise. However, the free surface, as an almost perfect reflector of energy, gives rise to high amplitude reflected waves that may be viewed as a 'secondary' sources. As a result the back-scattered modes, which have a greater sensitivity to the depth and dip of discontinuities, may be more useful for imaging than the forward-scattered P-s mode [*Nabelek et al.*, 1993; *Bostock et al.*, 2001; *Rondenay et al.*, 2001]. We will concentrate most of our attention on P-p-s, the stronger of the two back-scattered modes. The amplitudes of the scattered and reflected arrivals depend on backazimuth and incident angle, so availability of observations from a wide range of epicentral distances and backazimuths is essential to constructing a complete image of subsurface structure.

Prior to inversion the raw P-seisograms must be preprocessed to isolate the scattered displacement field from the incident wave field. This preprocessing prevents the source time history and near-source structure from being falsely mapped into receiver side structure. The preprocessing may be summarized as follows [see *Rondenay et al.*, 2001]:

1. Isolate the incident P wave by transforming displacement to wave vector space using the free-surface transfer matrix [*Kennett*, 1991].

2. Time normalize the resulting P wave section using multichannel cross-correlation-derived delay times [*VanDecar & Crosson*, 1990].

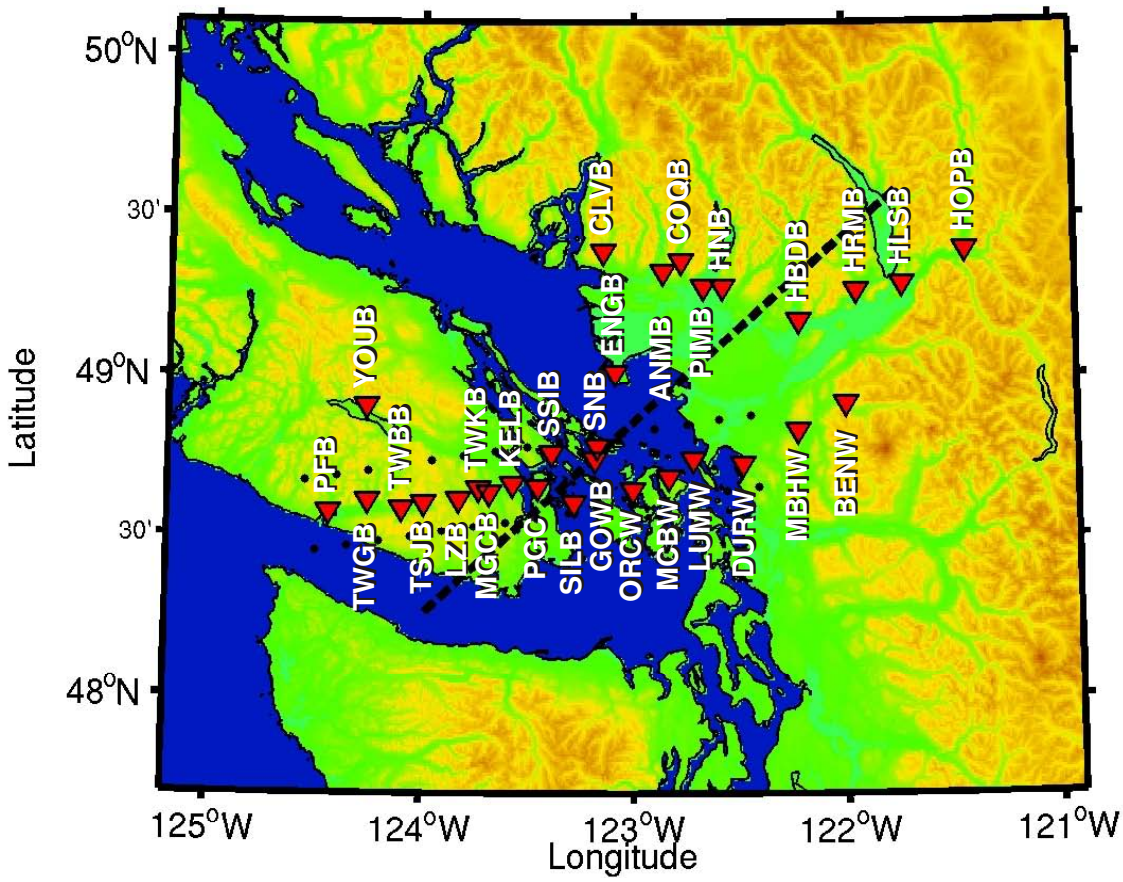

Figure 2: Distribution of broadband, three-component POLARIS-BC stations over northern Cascadia (red triangles). The dashed line shows the 2-D profile used in section 5 while the dotted region extending from PFB in the west to DURW in the east shows the region of seismicity used in figure 8.

3. Separate the incident and scattered wave fields by principal component analysis of the P wave section [*Ulrych et al.*, 1999].

4. Reconstitute scattered displacement using the inverse free-surface transfer matrix.

5. Deconvolve the incident source time function estimate from the recovered displacement sections.

6. Rotate horizontal displacement into a reference frame aligned with the inferred strike of the study area.

7. Filter the scattered displacement as required for 2-D Born inversion.

Figure 5 shows source-normalized scattered S-waves filtered between 0.3 and 0.03 Hz, for all seismograms in our data set. This scattering pattern is characteristic of a prominent, dipping low-velocity layer. Forward-scattered energy from a low-velocity dipping layer is clearly evident between 2 and 10 seconds as a negative (blue) pulse followed by a positive (red) pulse with minor moveout along the array. The blue-red-red-blue combination that dominates this seismogram section between 7 and 25 seconds from the east coast of Vancouver Island to

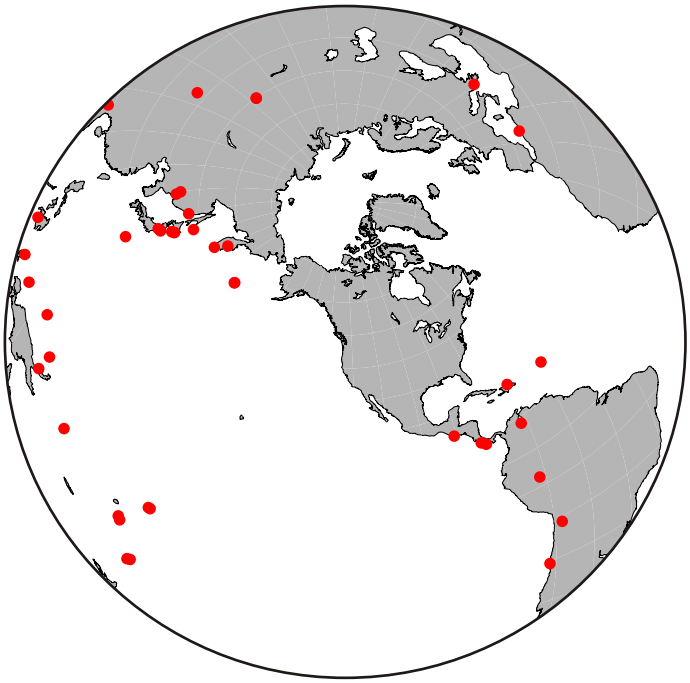

Figure 3: Distribution of events with sufficiently high signal to noise ratio. The region west of the array is well covered along with central and southern America. Note that, this distribution is reasonably good for a global teleseismic study.

approximately Lummi Island (LUM) in eastern Puget Sound/Georgia Strait is the combination of back-scattered P-p-s, the first negative (blue) and positive (red) pulse, and P-s-s modes, the second positive (red) and negative (blue) pulse. Both the forward- and back-scattered energy fades on stations to the east of Lummi Island.

There is also weaker energy that preceeds the forward-scattered P-s mode. This may indicate the presence of a shallower, weak, low-velocity zone that coincides with the C-reflection zone. Note that no coherent signal follows the back-scattered modes, indicating that any structure underlying the strong low-velocity zone must be must weaker. Also note that the first (blue) back-scattered pulse is very strong, indicating a large S-velocity contrast at the top of the low-velocity zone.

4 Neighbourhood inversion for multilayer structure

The first approach we take to modelling the data shown in figure 5 involves a non-linear inversion for the geometric and material properties of the subsurface structure. We use the ray theoretic forward-modelling algorithm of *Frederiksen & Bostock* [2000] wherein synthetic seismograms are generated for Earth models comprising stacks of planar, dipping layers. This forward modelling engine is employed within the neighbourhood inversion algorithm of *Sambridge* [1999] to efficiently search through a large ensemble of models and extract those that provide a close match to the data. The approach is applied in two ways - a multistation inversion, to determine the average layer geometry, and multiple inversions for single stations, to

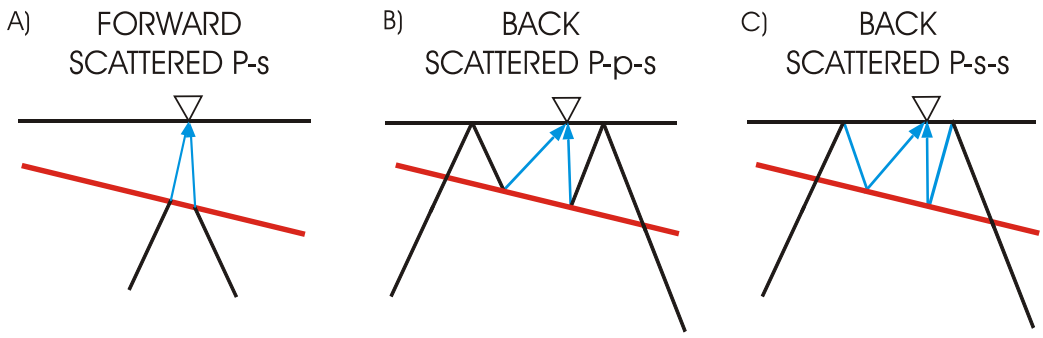

Figure 4: Scattering modes that can be clearly identified in the scattered wave field (e.g. figure 5). Ray paths from both an up-dip and a down-dip event are shown. The triangle represents the station and the red line a low-velocity layer. P-wave legs are shown in black and s-wave legs in blue. Note that up-dip and down-dip rays strike the low-velocity layer at markedly different angles.

allow the local structure beneath each station to be determined.

4.1 Multistation inversion

Cassidy & Ellis [1991] and *Cassidy* [1993] showed that the teleseismic response of subsurface structure beneath Vancouver Island is characterised by the C, E and F-layers that coincide with depth intervals of low S-velocity. Consequently, we model the subsurface structure as three dipping layers within a fixed background model. The variables in this inversion are the S-wave velocity within the C, E and F-layers and the depth, dip, strike and thickness of the layers. For simplicity, the strike of all three layers is constrained to be the same. The density within all layers is taken from *Clowes & Hyndman* [2002], as is the P-wave velocity of the C, E and F-layers. These P-wave velocities are similar to those found using receiver function analysis by *Cassidy & Ellis* [1993]. P- and S-velocities of all remaining layers are taken from the velocity model used by the Geological Survey of Canada (Cassidy pers. comm.) to locate earthquakes in the vicinity of Vancouver Island.

In the multistation inversion we use data from all stations labelled as dark blue triangles in figure 2. The best fit model for this inversion is provided in Table 1. Figure 5 shows the source-normalised scattered *S*-wave data used in this inversion along with synthetic versions generated using the best fit model. The main features of the observed scattered wave field are clearly reproduced in the synthetic seismograms. The dominant feature of this model is the large S-velocity contrast at the top and bottom of the E-layer. The top of this layer, at a depth of 22 km at PFB, dipping at deg 16.5, coincides with the top of the E-layer as imaged by *Green et al.* [1986]. The E-layer thickness of 4-5 km is also consistent with reflection data from this region [*Calvert et al.*, 1996; *Nedimovic et al.*, 2003]. Due to the use of data from an array of stations, the strike (Ndeg 48E) is likely to be better constrained than that determined from previous single station receiver function analysis. The S-wave velocity contrasts, of 1.1 km/s at the top and 1.45 km/s at the bottom of the E-layer, are consistent with the results of *Frederiksen* [2003], although they are larger than those proposed by *Cassidy* [1995].

The other two low-velocity layers (C and F) are significantly weaker than the E-layer. In particular, we note that the F-layer arises from the presence of slightly larger amplitude signals

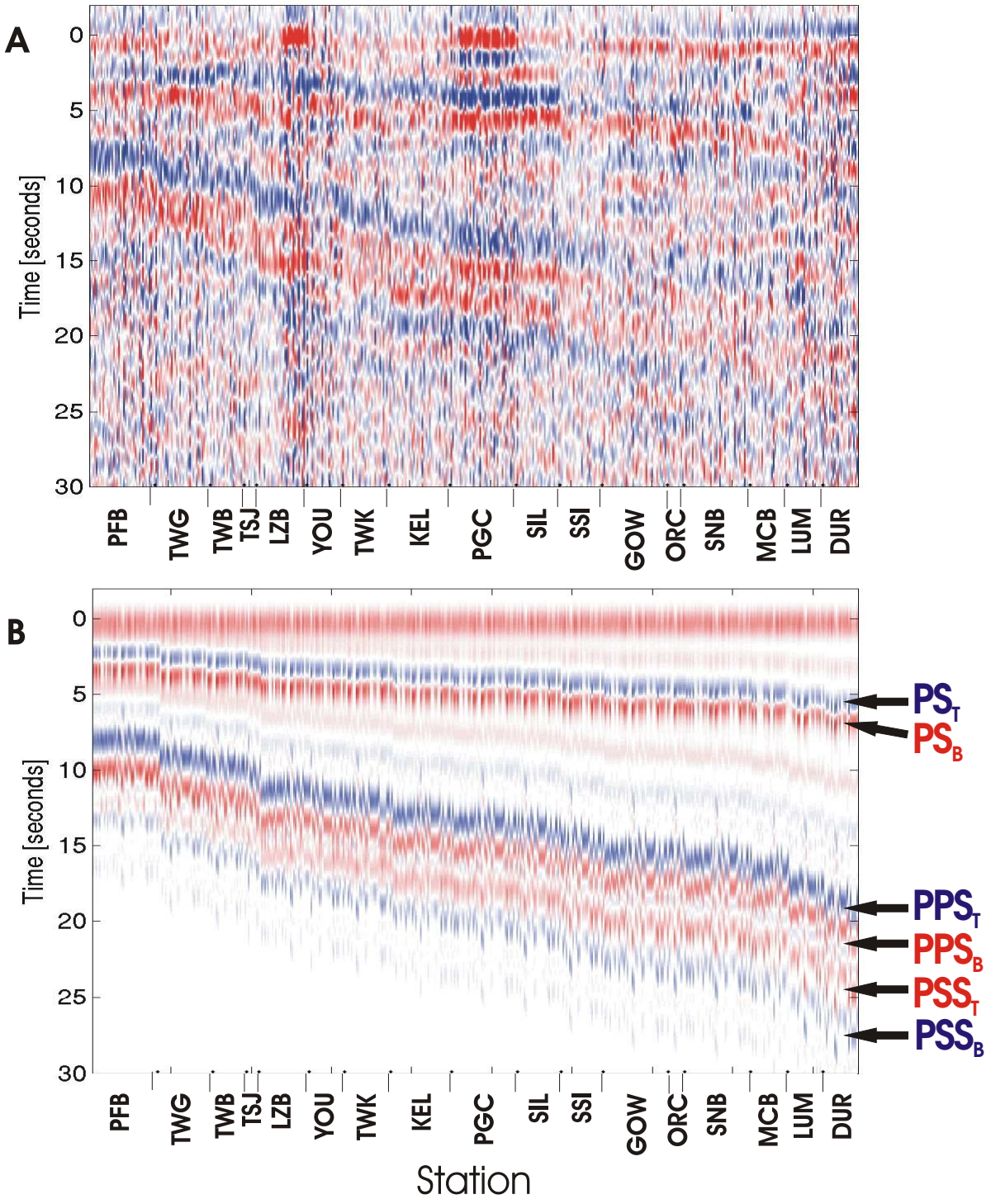

Figure 5: A) Source-normalized scattered *S*-waves for all the data used in the multistation neighbourhood inversion. B) Synthetic scattered *S*-waves generated using the best fit model (see Table 1). Stations are ordered by position along the profile with western station first. Note that the main features of the data are well reproduced by the synthetics. Also note that the correlated signal fades to the east of SSI. The polarity of the P-p-s mode is expected to be the opposite of that of the P-s-s mode, as is shown here.

Table 1: Model parameters for best fit plate model across Vancouver Island. Parameters for layers 1-3, 5 and 7 are held fixed in the inversion, as is the P- velocity and density for all layers.

Layer	Thickness (km)	V_P (m/s)	V_S (m/s)	ρ (kg m^{-3}	Strike	Dip
1	1.0	5000	2890	2800	0	0
2	5.0	6000	3460	2800	0	0
3	1.0	6700	3870	2930	0	0
4	4.0	6350	3790	2800	-48	9
5	11.0	7100	4100	3140	0	0
6	4.5	6350	2990	2800	-48	16.5
7	3.0	7750	4470	3030	0	0
8	5.0	6800	4280	2880	-48	17
9	90.0	7750	4470	3200	0	0

within the E-layer P-s-s window than expected (see figure 5) implying interference with an F-layer P-p-s phase. There is little or no visual indication of an F-layer P-s-s phase arriving at later times and removing the layer entirely only changes the fit to the data by a small amount (less than 1%), consistent with the results of *Frederiksen* [2003].

4.2 Single Stations Inversions

Inverting for the structure beneath individual stations allows the depth and material properties of layering to be determined locally near each station. Thus variations in V_S and deviations from planar layers can be investigated. Seventeen of the POLARIS-BC stations had sufficiently good signal-to-noise ratio and event coverage to allow single station inversions to be performed. The strike and dip of the layers is poorly constrained in single station inversions so we fix these values to agree with the multistation inversion.

Figure 6 shows the best fit models. As in the multistation inversion, the E-layer dominates these models with V_S contrasts of between 1.0 and 1.5 km.s^{-1} for most of the Vancouver Island stations followed by a weakening to between 0.5 and 1.0 km.s^{-1} beneath the San Juan Islands and the mainland. The thickness of the E-layer is approximately constant at 4 km across most of the array. The depth to the top of the E-layer is within 2 km of that predicted by the multistation inversion at all stations except YOUB, with no systematic trends. The depth at YOUB is 4 km shallower in the single station inversion because YOUB lies approximately 30 km to the north of the remainder of the array and the E-layer is known to shallow in this direction [*Green et al.*, 1986].

The C-layer is weak beneath most stations, but there is a consistent V_S increase beneath Vancouver Island stations of $\sim$0.5 km.s^{-1} at the base of the C-layer. An F-layer below the E-layer is apparent in the models for most stations, particularly those in central and eastern Vancouver Island, and coincides with the teleseismic F-layer inferred by *Cassidy* [1995] at station PGC (on the eastern side of Vancouver Island). As for the multistation analysis in section 4.1, the F-layer is generally required by the larger than expected signals within the E-layer P-s-s time window.

The only station where clear, correlated signal arrives after the E-layer P-s-s phase is KELB. The "receiver functions" for this station are shown in figure 7, ordered by event backazimuth.

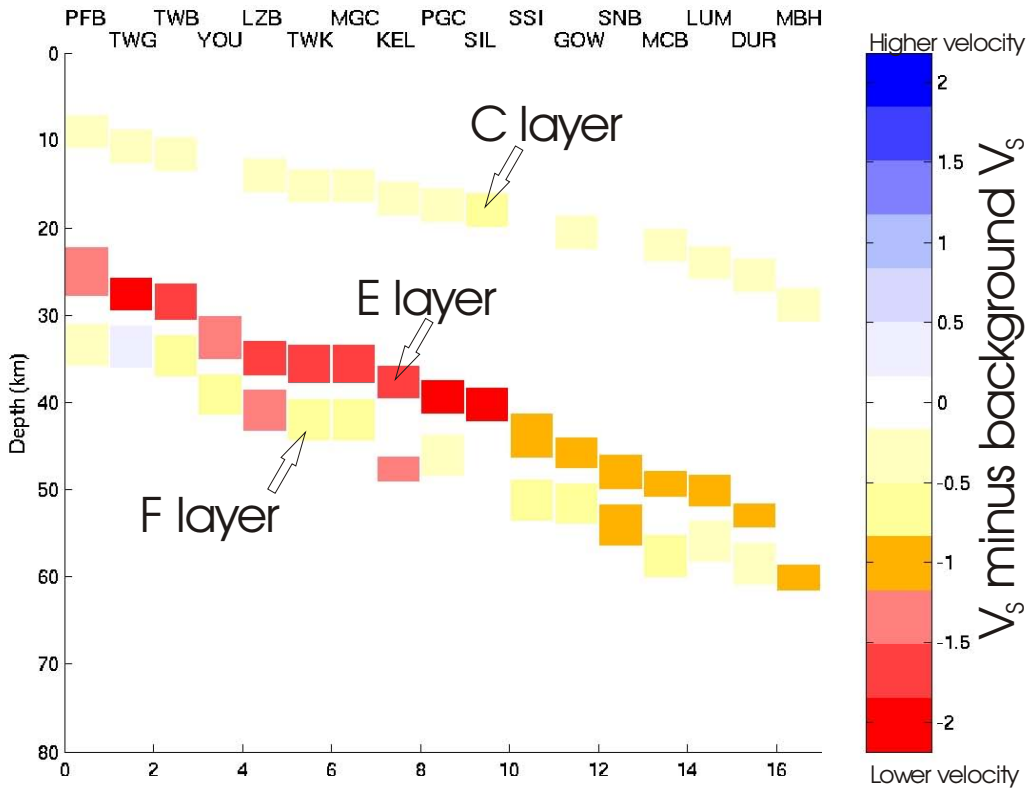

Figure 6: Results of single station neighbourhood inversions. The E-layer is the most prominent layer at all stations. However, many of the stations also show a low-velocity zone below the E-layer. Note that the depth of the continental Moho could not be reliably determined for this subset of stations so was not modelled in these inversions.

The signal of the E-layer is obvious across all source regions - between 3 and 5 seconds for forward-scattered P-s energy, 12 and 16 seconds for back-scattered P-p-s energy, and 16 and 20 seconds for back-scattered P-s-s energy. However, for events with backazimuths between deg 298 and deg 312 (i.e. those in Japan and Kamchatka) there is also correlated signal between 20 and 24 seconds. This feature would appear to be back-scattered P-s-s from a low-velocity layer 5-7 km below the E-layer. Note that the forward-scattered P-s energy and back-scattered P-p-s energy are obscured by interference with the E-layer P-s-s signal.

This observation can be explained in two ways:

1. There is a highly anisotropic, low V_S layer beneath the E-layer characterized by a strongly azimuthally dependent response, or,

2. There is an low V_S anomaly isolated to the northeast of KELB and below the E-layer.

We regard the former alternative as unlikely because no signal, of either the same or reversed polarity, is observed at other backazimuths, or at other stations, as would be expected for most classes of anisotropy. It is worth noting that the separation between the E-layer and the underlying anomaly is significantly greater for KELB than for the other stations. We have also considered the possibility that multiple anisotropic layers are involved but we have been unable

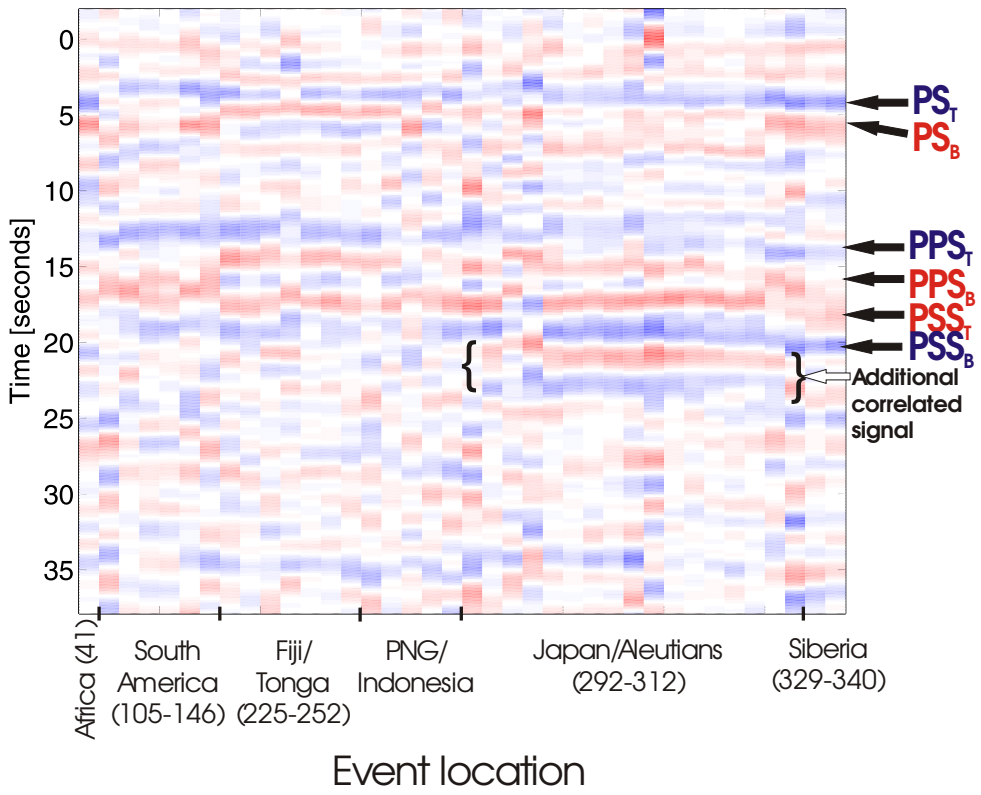

Figure 7: Source-normalized scattered S-waves for the station KELB ordered by back-azimuth. PS_T and PS_B denote the forward scattered arrivals from the top and bottom, respectively, of the low-velocity layer. PPS_T, PPS_B, PSS_T and PSS_B denote similar arrivals for the backscattered P-p-s and P-s-s modes. The back-azimuth ranges for the source regions are shown in brackets.

to reproduce the narrow backazimuth range of the observed correlated signal. Therefore we conclude that correlated signal between 20 and 24 seconds in figure 7 is caused by a localized, low V_S anomaly to the northeast of KELB.

In summary then, the single station inversions indicate:

1. The E-layer is the most prominent low-velocity layer across the whole study region.

2. The E-layer is more prominent beneath Vancouver Island than beneath the San Juan Islands or the lower mainland.

3. The E-layer does not deviate significantly from a planar structure along the linear portion of the array, but shallows to the north of the array.

4. There may be a weak low-velocity zone below the E-layer. If so, it parallels the E-layer and there is a clear separation between the top of it and the bottom of the E-layer of $\sim$1.5 km.

5 Two-dimensional Migration Inversion

We now proceed to a simultaneous 2-D linearized inversion/migration of the same data set. For this application we use the strike direction of the dipping plate from Table 1 to map the stations onto a cross strike linear profile. We use the inversion algorithm of *Bostock et al.* [2001] that allows seismograms from events at arbitrary backazimuths to be inverted under the assumption that the underlying structure perpendicular to the profile is invariant. This approach has the advantage that imaged structures are not constrained to be planar but can assume arbitrary geometry within the restriction of 2-dimensionality.

The approach is based on high-frequency and single-scattering approximations and casts the inverse problem as a generalized Radon transform. An image is produced for each of the main scattering modes. However, we will concentrate on the back-scattered P-p-s mode because our investigation, and that of *Rondenay et al.* [2001], found this mode to provide the strongest structural signature. As above, we have cast our inversion in terms of the recovery of S-velocity perturbations. A background model is required that accurately accounts for the propagation characteristics of the incident and scattered wavefields. For this purpose we again use the 1-D model employed by the Geological Survey of Canada in their earthquake relocations, as specified in layers 1-3, 5 and 7 in Table 1.

Figure 8 shows the results of the inversion. Two of the features in this image are artifacts. First, the migration "smiles" at the eastern end of the profile are the result of poor station coverage at this end of the array and highly reverbatory responses caused by strong variations in tomography and velocity in the upper Fraser Valley. The signature of these reverberations diminishes at lower frequencies (see figure 9A). Secondly, the low-velocity zones between 5-10 km depth and 40-80 km depth are the result of mis-migrated forward-scattered P-s and back-scattered P-s-s arrivals. These artificial low-velocity zones were also clear in a corresponding image from the study of *Rondenay et al.* [2001], shown in figure 9B.

Several legitimate structural features are also obvious in figure 8. At the western edge of the profile a prominent, dipping low-velocity zone is clear between two higher velocity zones. This low-velocity zone has the same dip and depth as the prominent low-velocity zone identified in sections 4.1 and 4.2, and previous estimates of the position of the E-layer [*Green et al.*, 1986]. The thickness of this layer, which is slightly overestimated due to interference between the backscattered modes, provides an upper-limit on the true thickness of 6-8 km. As shown in section 4.2, the E-layer is most prominent beneath Vancouver Island and its signature fades beneath the San Juan Islands.

The continental Moho can be seen as a low-velocity region overlying a higher velocity region in the western 100 km of the profile. The depth of this transition ($\sim$38 km) is consistent with the results of *Zelt et al.* [1993], who used seismic refraction data to estimate a Moho depth of 37 km at the eastern end of our profile. The contrast at this interface diminishes in the easterly direction and disappears completely approximately 130 km along the profile. As in Oregon [*Bostock et al.*, 2002], we interpret this disappearance of a clear continental Moho interface near the centre of the profile to indicate the presence of a serpentinized forearc mantle, which gives rise to a significantly reduced velocity contrast across the continental Moho.

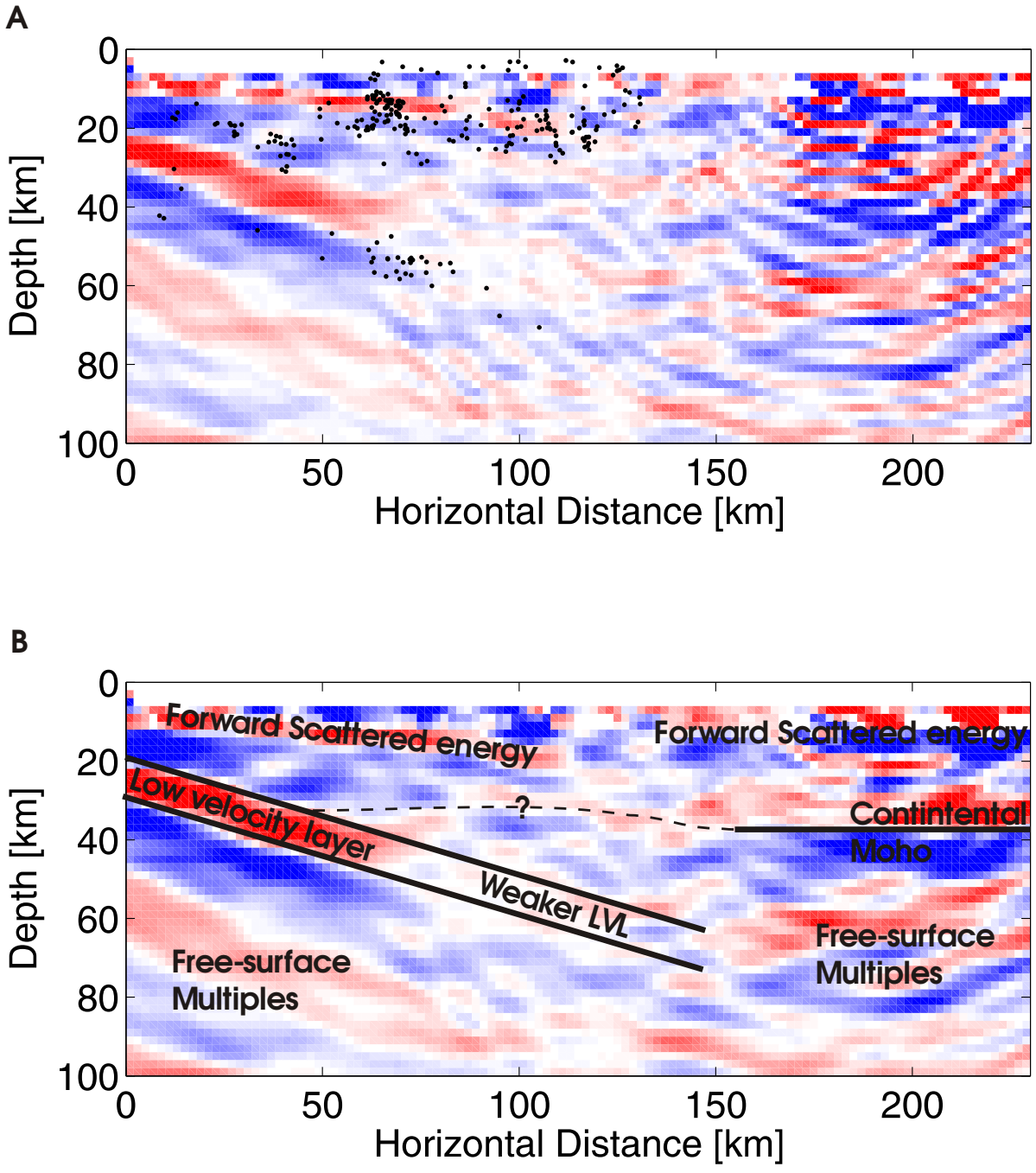

Figure 8: A) Teleseismic migration image using the scattered P-p-s phase across Vancouver Island, northwestern Washington and the British Columbia lower mainland. Red and blue regions indicate low and high S-velocity respectively. The frequency range of the "receiver functions" used is in these inversions is 0.5-0.03 Hz. Circles represent the hypocentres of earthquakes recorded near the POLARIS-BC array. B) Lower frequency version overlain with interpretation of features.

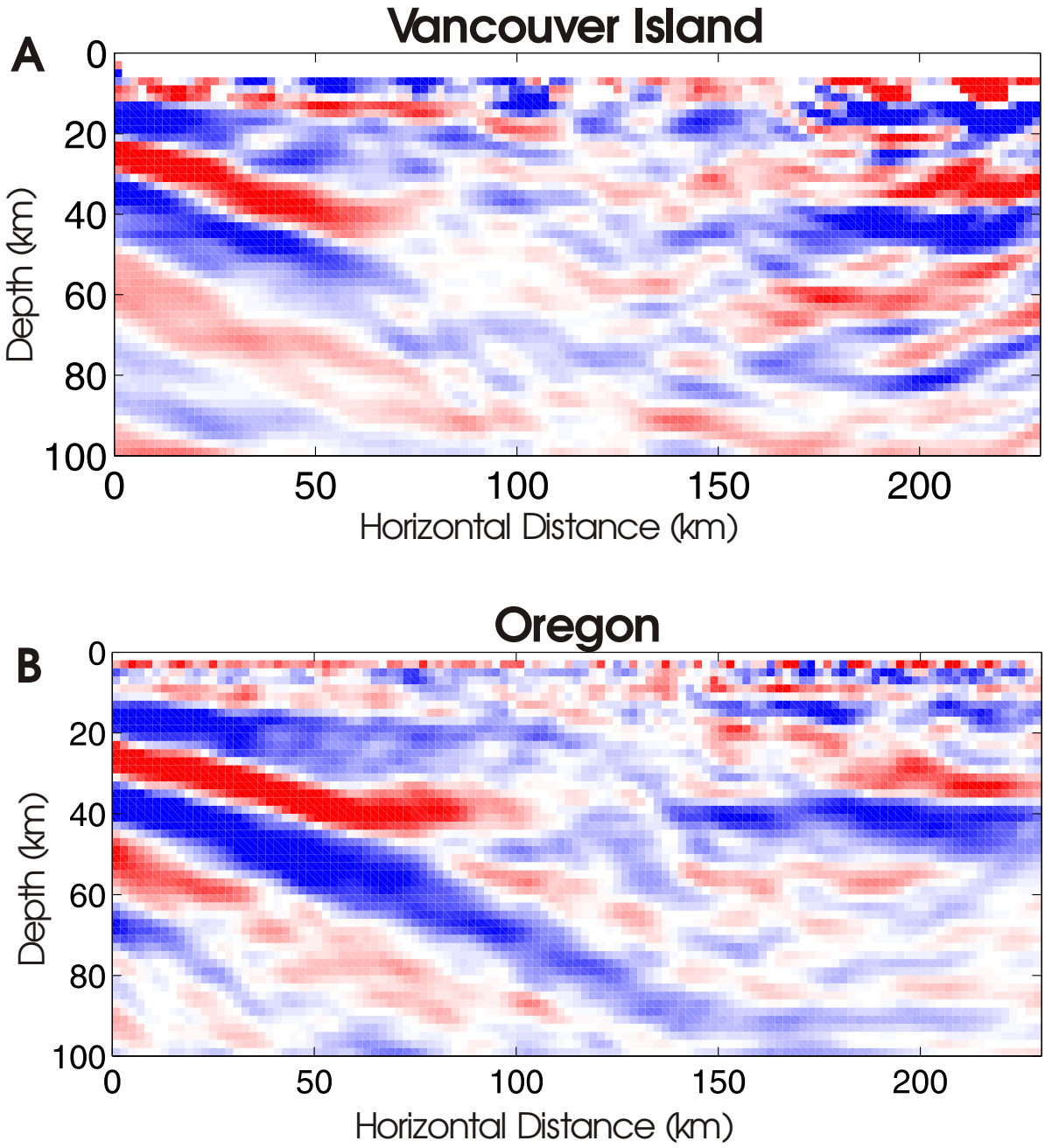

Figure 9: Same as figure 9 with the frequency range limited to 0.3-0.03 Hz. A) Vancouver Island, B) Oregon (Rondenay et al. 2001).

6 Discussion and Conclusions

Similar studies of subduction zones elsewhere using scattered teleseismic P-waves, notably Alaska [*Ferris et al.*, 2003; *Abers et al.*, 2002; Kamchatka [*Yuan et al.*, 1999; *Levin et al.*, 2002], South America [*Bock et al.*, 2000; *Yuan et al.*, 2000] and southern Cascadia [*Rondenay et al.*, 2001], have revealed the presence of a prominent dipping, low S-velocity layer associated with the subducting plate. This feature is, in many cases, closely associated with shallow Wadati-Benioff seismicity and is apparent over a wide range of depths; it can be traced to depths well below crustal levels (∼150 km) in the colder thermal regimes of the Andes [*Yuan et al.*, 2000] and Alaska [*Ferris et al.*, 2003]. The depth extent of the teleseismic low-velocity E-layer in Cascadia is best ascertained through examination of individual record sections. Figure 10 shows receiver functions for an event in Kamchatka on June 16th 2003. As in figure 5, the signal from the low-velocity layer is clear, particularly for the backscattered modes (8-25 seconds). From these data we can conclude that the low-velocity layer extends at least as far east as the mainland stations DUR and ANM, and to depths of 60-65 km. This observation is consistent with the results of a seismic reflection study on Texada Island (just north of our profile), as well as the results of a reflection experiment 150 km further south in the Puget Sound, which indicated that the E-layer extends into the mantle (> 50 km) [*Clowes*, pers. comm.; *Calvert et al.*, 2003]. We can conclude from these observations that the E-layer is not restricted to crustal depths, but persists well into the mantle along strike over a wide region while retaining much of its low velocity/high reflectivity character.

An image of short wavelength S-velocity structure beneath Oregon [*Rondenay et al.*, 2001] determined using the same approach as employed in section 5 is shown in figure 9B. There is a close correspondence between the major subsurface features along the Vancouver Island and Oregon profiles. In particular, a prominent low-velocity zone is apparent between depths of 20 km and 40 km, extending approximately 100 km along the profile. The thickness and geometry of this layer are similar in both images as is the reduction in strength of the feature at greater depths. We can reasonably argue, therefore, that the low-velocity zone represents either the same structural feature in both cases or two different tectonic structures that produce very similar S-velocity signatures. Given that the two profiles cross the same subduction zone and are separated by only ∼500 km along strike we shall discount the latter alternative. We are left with the conclusion that the low-velocity zone manifests the same fundamental structure in both locations. However, beneath Oregon the low-velocity zone has been ascribed to subducted oceanic crust [*Nabelek et al.*, 1993; *Rondenay et al.*, 2001], whereas beneath Vancouver Island it is identified as part of the overriding plate (the E-layer) approximately 5-10 km above the oceanic crust [*Cassidy & Ellis* 1991]. There are two obvious ways of reconciling this contradiction:

1. the low-velocity zone is oceanic crust, which is then shallower beneath Vancouver Island than previously thought, or;

2. the low-velocity zone is not oceanic crust and the subducting plate beneath Oregon is significantly deeper than previously thought.

In either case, the interpreted depth to the plate boundary along the Cascadia margin requires reconsideration. We now explore the further evidence that may help distinguish between these alternatives.

In addition to the receiver function studies identified above, the presence of a low-velocity layer in subduction zones with a thickness of order ∼10 km has been supported by analysis of

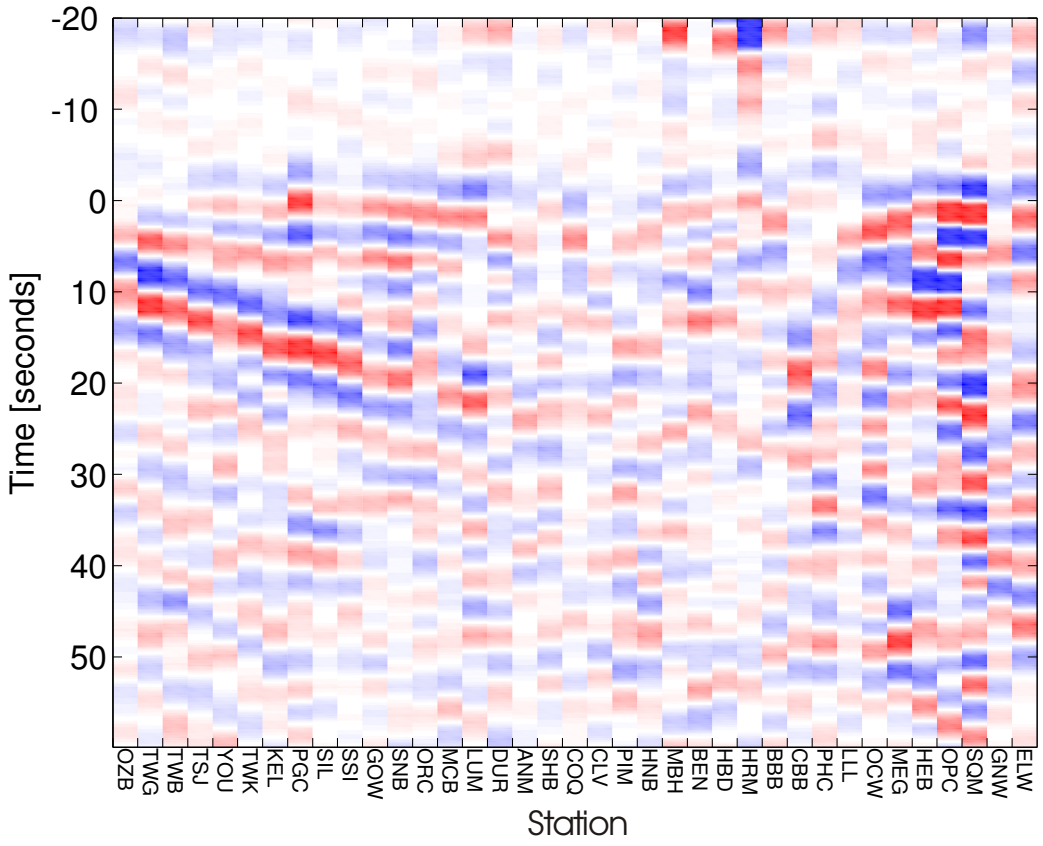

Figure 10: Source-normalized scattered S-waves for an a magnitude 6.3 event in Katchatka on June 16th, 2003.

the move-out of local P-S converted phases in Japan [*Matsuzawa et al.*, 1986] and the eastern Aleutians [*Helffrich & Abers*, 1997] and by analysis of the dispersion of seismic body waves from slabs beneath Alaska, the central Aleutians, the northern Kuriles, northern Japan and the Marianas [*Abers et al.*, 1996; *Abers*, 2000]. From the compilation of these data, *Hacker et al.* [2003], in agreement with *Ferris et al.* [2003], [Yuan et al. [2000] and *Rondenay et al.* [2001], draw the conclusion that the low-velocity zone is subducted oceanic crust. Furthermore, beneath Oregon, the position of the low-velocity zone imaged by *Rondenay et al.* [2001] agrees with independent estimates for the position of the crust derived from controlled-source seismic surveys using refracted phases and wide-angle reflections [*Trehu et al.* [1994]. On the basis of the broad consistency of these observations and interpretations we shall proceed under the hypothesis that the prominent low-velocity zones beneath Oregon and Vancouver Island represent subducted oceanic crust, and examine the implications for earlier work on structure of the slab in the northern region. An association of the E-layer with subducting oceanic crust implies that the position of the subducting Juan de Fuca plate beneath Vancouver Island is 8-10 km shallower than that proposed *e.g.* by *Hyndman et al.* [1990] and others, and 4-5 km shallower than that proposed by *Nedimovic et al.* [2003]. This interpretation is also consistent with the observation that the low-velocity layer/E-layer extends to mantle depths of at least 60-65 km in Northern Cascadia. We interpret the low-velocity character of this layer to be caused primarily by the presence of water released and largely trapped within the subducting oceanic crust as

it encounters higher temperatures and pressures. We suggest, in turn, that the released free water may lead to the formation of thin, dipping, fluid filled lenses of high porosity within the oceanic crust giving rise to the high reflectivity associated with this layer, similar to the mechanism proposed by *Hyndman* [1988], but within the subducting plate not the overriding continental plate]. Thus the teleseismic signature of the E-layer manifests an overall S-velocity reduction within the oceanic crust due to the presence of free water, whereas the E-reflectors observed in active source studies are generated by highly localized zones of water saturation. In regions where water can escape into the overlying continental plate, similar reflectivity may be generated, thereby explaining the variability in thickness of the E-layer observed to the south [*Calvert et al.* [2003].

6.1 Active Source Seismic Studies

Previous interpretations [*e.g. Hyndman et al.*, 1990; *Clowes et al.*, 1995; *Calvert & Clowes*, 1990; *Nedimovic et al.*, 2003] based upon seismic reflection and refraction data have associated the top or bottom of the oceanic crust with the F-reflector. This reflection is weak and sufficiently difficult to trace beneath Vancouver Island that the initial interpretations of the Lithoprobe profile originally assigned the E-layer to the oceanic crust and did not identify any major features below this level. The interpretation of the F-reflector as the top or bottom of the crust beneath Vancouver Island relies, in part, on the extrapolation of the top of oceanic crust offshore, where it is clearly identifiable on marine reflection sections seaward of the deformation front, to the onshore profiles. Below the deformation front, the reflection from top of crust can no longer be traced with confidence and spatially coherent reflections are difficult to identify, due in part to large lateral velocity variations within the top 3-4 km of overlying crust [*e.g. Nedimovic et al.*, 2003]. The F-reflector represents a weak and highly intermittent set of reflector segments beneath the shelf and the difficulties in accurately tracing it through to the coast line are highlighted by the conflicting interpretations of *Clowes et al.* [1995], *Hyndman et al.* [1990], *Calvert & Clowes* [1990], and *Nedimovic et al.* [2003]. Constraints on the location of subducting crust based on seismic refraction data have also been called into question recently. *McNeill & Spence* [pers. comm., 2004] have reinterpreted seismic refraction data from 1980 across central Vancouver Island and argue that a shallower plate is consistent with the observations. Thus, there appears to be sufficient latitude within the constraints supplied by active source seismic data to re-identify the E-layer beneath Vancouver Island with subducted oceanic plate and thereby retain consistency with the teleseismic results.

6.2 Seismicity

Previous estimates on the position of the subducting oceanic crust have also been constrained by the location of shallow Wadati-Benioff seismicity [*e.g.*[*Green et al.*, 1990; *Hyndman et al.*, 1990; *Nedimovic et al.*, 2003]. These studies assume that seismicity is related to metamorphic reactions taking place within the oceanic crust as it encounters higher temperatures and greater pressures [*Hacker et al.* [2003]. Recently, however, *Preston et al.* [2003] have used regional, P-traveltime tomography of refraction and wide-angle reflection data and precisely relocated hypocenters to argue that shallow (20-45 km) Wadati-Benioff seismicity further to the south below the Olympic Peninsula and northwest Washington State actually occurs with the subducted oceanic mantle up to the oceanic Moho and is the result of dehydration embrittlement of mantle serpentine.

Figure 8 shows the location of magnitude 1.0 and larger events that have occurred between 1986 and 1998 within the region defined by the dotted square in figure 2. These locations were provided by the Geological Survey of Canada and were located using the same background velocity models as we used in sections 4 and 5. The majority of Wadati-Benioff events on this profile occurred beneath the east coast of Vancouver Island at depths between 40 and 60 km. Given the uncertainty in velocity models, hypocenter locations and projection of locations onto the 2-D profiles, the hypocenter distribution in figure 8 is broadly similar to that shown in figure 2 of Preston et al (2003) if we take the low-velocity E-layer, as determined teleseismically, to coincide with the oceanic crust. Under this interpretation, weakly defined seismic structures below the oceanic Moho, namely the F-reflectors and the weak low-velocity F-layer identified by *Cassidy* [1995] and evident in table 1 and figure 6, can be ascribed to locally generated metamorphic dehydration fronts within the oceanic plate mantle, specifically, due to the serpentinite to peridotite reaction [*Preston et al.*, [2003]. It should also be noted that, despite significant differences in thermal structure, a similar distribution of earthquakes relative to a highly reflective subducting oceanic crust has been interpreted beneath the Andes [*Oncken et al.*, 1999].

7 Conclusions

In this paper we have documented the presence of a prominent dipping, low S-velocity layer extending from the west coast of Vancouver Island eastward to beyond the east coast of Georgia Strait/Puget Sound. This feature coincides with the E-reflection layer identified in near-vertical seismic reflection profiles and has a character similar to low-velocity layers observed teleseismically in other parts of the world. Although the E-layer is most prominent at depths of 20-40 km depth below Vancouver Island, its high reflectivity-low velocity signatures persist to depths of >50 km beneath the British Columbia mainland and northwest Washington. We have argued that the low-velocity layer observed teleseismically in this and a comparable study in Oregon represent the same tectonic feature, thus implying that current views on the position of the subducting plate are incorrect in one of the two regions. The broad consistency of teleseismic results from a range of subduction zones, the similarities in structure between the Vancouver Island and Oregon profiles, and the extension of the low-velocity E-layer well into mantle depths collectively support the thesis that the E-layer does not reside within the continental crust but, rather, forms part of the downgoing plate as interpreted in early LITHOPROBE studies. More specifically, we propose that the low-S velocity layer defines the subducting oceanic crust of the Juan de Fuca plate. This interpretation implies that the position of the subducting Juan de Fuca crust beneath Vancouver Island is 8-10 km shallower than that proposed *e.g.* by *Hyndman et al.* [1990] and others, and 4-5 km shallower than that proposed by *Nedimovic et al.* [2003].

8 Publications stemming from this research

Nicholson, T., Bostock, M.G., and Cassidy, J., (2004). New constraints on subduction zone structure in northern Cascadia, *submitted to Geophys. J. Int.*, July 2004.

9 References

Abers, G. A., (2000). Hydrated subducted crust at 100-250 km depth, *Earth Planet. Sci. Lett.*, **176**, 323-330.

Abers, G. A., and Sarker, G., (1996). Dispersion of regional body waves at 100-150 km depth beneath Alaska: In situ constraints on metamorphism of subducted crust, *Geophys. Res. Lett.*, **23**, 1171-1174.

Abers, G. A., Stachnik, J., Pozgay, S., Christensen, D. H., Hansen, R., and Meyers, E. V., (2002). The BEAAR facts: Sampling the Alaskan slab, wedge and mountains with a broadband experiment across Alaska Range (BEAAR), *Seismol. Res. Lett.*, **73**, 219.

Bock, G., Schurr, B. and Asch, G., (2000). High-resolution image of the oceanic Moho in the subducting Nazca plate from P-S converted waves, *Geophys. Res. Lett.*, **27**, 3929-3932.

Bostock, M. G., Hyndman, R. D., Rondenay, S. and Peacock, S. M., (2002). An inverted continental Moho and serpentinization of the forearc mantle, *Nature*, **417**, 536-538.

Bostock, M. G., Rondenay, S. and Shragge, J., (2001). Multiparameter two-dimensional inversion of scattered teleseismic body waves 1. Theory for oblique incidence, *J. Geophys. Res.*, **106**, 30771-30782.

Calvert, A. J. and Clowes, R. M., (1990). Deep, high amplitude reflections from a major shear zone above the subducting Juan de Fuca plate, *Geology*, **18**, 1091-1094.

Calvert, A. J., (1996). Seismic reflection constraints on imbrication and underplating of the northern Cascadia convergent margin, *Can. J. Earth Sci.*, **33**, 1294-1307.

Calvert, A. J., Fisher, M. A., Ramachandran, K. and Trehu, A. M., (2003). Possible emplacement of crustal rocks into the forearc mantle of the Cascadia Subduction Zone, *Geophys. Res. Lett.*, **30**, 2196, doi:10.1029/2003GL018541.

Calvert, A. J., (2004). Seismic reflection imaging of two megathrust shear zones in the northern Cascadia subduction zone, *Nature*, **428**, 163-167.

Cassidy, J. F. and Ellis, R. M., (1991). Shear wave constraints on a deep crustal reflective zone beneath Vancouver Island, *J. Geophys. Res.*, **96**, 19,843-19,851.

Cassidy, J. F. and Ellis, R. M., (1993). S wave velocity structure of the Northern Cascadia subduction zone, *J. Geophys. Res.*, **98**, 4407-4421.

Cassidy, J. F., (1995). A comparison of the receiver structure beneath stations of the Canadian National Seismograph Network, *Can. J. Earth Sci.*, **32**, 938-951.

Cassidy, J. F. and Waldhauser, F., (2003). Evidence for both crustal and mantle earthquakes in the subducting Juan de Fuca plate, *Geophys. Res. Lett.*, **30**(2), 1095, doi:10.1029/2002GL015511.

Clowes, R. M., Baird, D. J. and Dehler, S. A., (1997). Crustal structure of the northern Cascadia subduction zone, southwestern British Columbia, from potential field and seismic studies, *Can. J. Earth Sci.*, **34**, 317-335.

Clowes, R. M., Brandon, M. T., Green, A. G., Yorath, C. J., Sutherland Brown, A., Kanesewich, E. R. and Spencer, C., 1987. LITHOPROBE - southern Vancouver Island: Cenozoic subduction complex imaged by deep seismic reflections, *Can. J. Earth Sci.*, **28**, 542-556.

Clowes, R. M., Zelt, C. A., Amor, J. R. and Ellis, R. M., (1995). Lithospheric ctructure in the southern Canadian Cordillera from a network of seismic refraction lines, *Can. J. Earth Sci.*, **32**, 1485-1513.

Clowes, R. M. and Hyndman, R. D., (2002). Geophysical Studies of the Northern Cascadia Subduction Zone off Western Canada and their Implications for Great Earthquake Seismotectonics: A Review, In Fujinawa, Y. and Yoshida, A. (Eds.), *Seismotectonics in Convergent Plate Boundary*, pp. 1-23, Terra Scientific Publishing, Tokyo, Japan.

DeMets, C., Gordon, R. G., Argus, D. F. and Stein, S., (1990). Current plate motions, *Geophys. J. Int.*, **101**, 423-478.

Dragert, H., Wang, K. L. and James, T. S., (2001). A silent slip event on the deeper Cascadia Subduction interface, *Science*, **292** (5521), 1525-1528.

Drew, J. J. and Clowes, R. M., (1990). A re-interpretation of the seismic structure across the active subduction zone of western Canada, In Green, A. G. (Ed.), *Studies of Laterally Heterogeneous Structures Using Seismic Refraction and Reflection Data*, *Geol. Surv. Can.*, Paper 89-13, 115-132.

Engebretson, D. C., Kelley, K. P., Cashman, H. J. and Richards, M. A., (1992). 180 million years of subduction, *GSA Today*, **2**, 93-95.

Ferris, A., Abers, G. A., Christensen, D. H. and Veenstra, E., (2003). High resolution image of the subducted Pacific (?) plate beneath central Alaska, 50-150 km depth, *Earth and Planet. Sci. Lett.*, **214**, 575-588.

Frederiksen, A. W. and Bostock, M. G., (2000). Modelling teleseismic waves in dipping anisotropic structures, *Geophys. J. Int.*, **141**, 401-412.

Frederiksen, A. W., Folsom, H. and Zandt, G., (2003). Neighbourhood inversion of teleseismic Ps conversions for anisotropy and layer dip, *Geophys. J. Int.*, **155**, 200-212.

Green, A. G., Clowes, R. M., Yorath, C. J., Spencer, C., Kanesewich, E. R., Brandon, M. T. and Sutherland Brown, A., (1986). Seismic reflection imaging of the subducting Juan de Fuca plate, *Nature*, **319**, 210-213.

Green, A. G., Clowes, R. M. and Ellis, R. M., (1990). Crustal studies across Vancouver Island and adjacent offshore margin, In Green, A. G. (Ed.), *Studies of Laterally Heterogeneous Structures Using Seismic Refraction and Reflection Data*, *Geol. Surv. Can.*, 3-25.

Hacker, B. R., Peacock, S. M., Abers, G. A. and Holloway, S. D., (2003). Subduction factory, 2, Are intermediate-depth earthquakes in subducting slabs linked to metamorphic dehydration reactions?, *J. Geophys. Res.*, **108**B1, 2030, doi:10.1029/2001JB001129.

Hasselgren, E. O. and Clowes, R. M., (1995). Crustal structure of northern Juan de Fuca plate from multichannel reflection data, *J. Geophys. Res.*, **100**, 6469-6486.

Helffrich, G., and Abers, G., A., (1997). Slab low-velocity layer in the eastern Aleutian subduction zone, *Geophys. J. Int.*, **130**, 640-648.

Hyndman, R. D., (1988). Dipping seismic reflectors, electrically conductive zones, and trapped water in the crust over a subducting plate, *J. Geophys. Res.*, **93**, 13,391-13,405.

Hyndman, R. D., Yorath, C. J., Clowes, R. M. and Davis, E. E., (1990). The northern Cascadia subduction zone at Vancouver Island: seismic structure and tectonic history, *Can. J. Earth Sci.*, **27**, 313-329.

Hyndman, R. D., and Wang, K., (2003). Thermal constraints on the zone of major thrust earthquake failure - the Cascadia Subduction zone, *J. Geophys. Res.*, **98**, 2039-2060.

Kennett, B. L. N., (1991). Removal of free surface interactions from three-component seismograms, *J. Geophys. Int.*, **104**, 153-163.

Kurtz, R. D., De Laurier, J. M. and Gupta, J. C., (1986). A magnetotelluric sounding across the subducting Juan de Fuca plate, *Nature*, **321**, 596-599.

Langston, C. A., (1979). Structure under Mount Rainier, Washington, inferred from teleseismic body waves, *J. Geophys. Res.*, **84**, 4749-4762.

Levin, V., Park, J., Brandon, M., Lees, J., Peyton, V., Gordeev, E. and Ozerov, A., (2002). Crust and upper mantle of Kamchatka from teleseismic receiver functions, *Tectonophysics*, **358**, 233-265.

Matsuzawa, T., Umino, N., Hasegawa, A., and Takagi, A., (1986). Normal fault type events in the upper plane of the double-planed deep seismic zone beneath the northeastern Japan Arc, *J. Phys. Earth*, **34**, 85-94.

McNeill, A. F. and Spence, G. D., (2004). A Re-interpreted Seismic velocity model beneath Vancouver Island, Canada: a shallower subducting slab?, *Eos Trans. AGU*, Spring Meet. Suppl.

Nabelek, J., Li, X. Q., Azevedo, S., Braunmiller, J., Fabritius, A., Leitner, B., Trehu, A. M. and Zandt, G., (1993). A high-resolution image of the Cascadia subduction zone from teleseismic converted phases recorded by a broadband seismic array, *Eos Trans. AGU*, **74**(43), Fall Meet. Suppl., 431.

Nedimovic, M. R., Hyndman, R. D., Ramachandran, K. and Spence, G. D., (2003). Reflection signature of seismic and aseismic slip on the northern Cascadia subduction interface, *Nature*, **424**, 416-420.

Nicholson, T., Sambridge, M. and Gudmundsson, O., (2002). Hypocentre location by pattern recognition, *J. Geophys. Res.*, **107**, doi:10.1029/2000JB000035.

Nicholson, T., Sambridge, M. and Gudmundsson, O., (2004). Three-dimensional empirical traveltimes: construction and application, *Geophys. J. Int.*, **156**, 307-328, doi: 10.1111/j.1365-246X.2003.02137.x.

Oncken, O., Luschen, E., Mechie, J., Sobolev, S., Schulze, A., Gaedicke, C., Grunewald, S., Bribach, J., Asch, G., Giese, P., Wigger P., Schmitz, M., Lueth, S., Scheuber, E., Haberland, C., Rietbrock, A., Gotze, HJ., Brasse, H., Patzwahl, R., Chong, G., Wilke, H.G., Gonzalez, G., Jensen, A., Araneda, M., Vieytes, H., Behn, G., Martinez, E., Rossling, R., Amador, J., Ricaldi, E., Chumacero, H., and Luterstein, R., (1999). Seismic reflection image revealing offset of Andean subduction-zone earthquake locations into oceanic mantle, *Nature*, **397**(6717), 341-344.

Preston, L. A., Creager, K. C., Crosson, R. S., Brocher, T. M. and Trehu, A. M., (2003). Intraslab Earthquakes: Dehydration of the Cascadia Slab, *Science*, **302**, 1197-1200.

Ramachandran, K., (2001). Velocity structure of SW British Columbia and NW Washington from 3-D non-linear seismic tomography. PhD thesis, Univ. Victoria, 1-198.

Riddihough, R. P., (1982). One hundred million of plate tectonics in western Canada, *Geosci. Can.*, **9**, 28-34.

Riddihough, R. P. and Hyndman, R. D., (1991). The modern plate tectonic regime of the continental margin of western Canada, In Gabrielse, H. and Yorath, C. J. (Eds.), *Geology of the Cordilleran Orogen in Canada*, *Geol. Surv. Can.*, *Geology of Canada*, **2**, 435-455.

Rogers, G. and Dragert, H., (2003). Episodic tremor and slip on the Cascadia subduction zone: The chatter of silent slip, *Science*, **300**(5627), 1942-1943.

Rondenay, S., Bostock, M. G. and Shragge, J., (2001). Multiparameter two-dimensional inversion of scattered teleseismic body waves 3. Application to the Cascadia 1993 data set, *J. Geophys. Res.*, **106**, 30795-30807.

Sambridge, M. S., (1999). Geophysical inversion with a neighbourhood algorithm - I. Searching a parameter space, *Geophys. J. Int.*, **138**, 479-494.

Tréhu, A. M., Asudeh, I., Brocher, T. M., Luetgert, J. H., Mooney, W. D., Nabelek, J. L., and Nakamura, Y., (1994). Crustal architecture of the Cascadia forearc, *Science*, **266**, 237-243.

Ulrych, T. J., Friere, S. L. M., and Sacchi, M. D., (1999). Eigenimage processing of seismic sections, In Kirlin, R. L. and Done, W. J. (Eds.), *Covariance Analysis for Seismic Signal Processing*, Soc. of Explor. Geophys., Tulsa, Oklahoma.

VanDecar, J. C., and Crosson, R. S., (1990). Determination of teleseismic relative phase arrival times using multi-channel cross-correlation and least squares, *Bull. Seismol. Soc. Am.*, **80**, 150-159.

Waldhauser, F. and Ellsworth, W. L., (2000). A double-difference location algorithm: Method and application to the northern Hayward fault, *Bull. Seism. Soc. Am.*, **90**, 1353-1368.

Wang, C. X., (1997). Structure of the Cascadia subduction zone off Vancouver Island: New evidence from seismic refraction data, *Masters Thesis*, Univ. British Columbia.

Yamauchi, M., Hirahara, K. and Shibutani, T., (2003). High resolution receiver function imaging of the seismic velocity discontinuities in the crust and uppermost mantle beneath southwest Japan, *Earth Planet. Sci. Lett.*, **55**(1), 59-64.

Yorath, C. J., Green, A. G., Clowes, R. M., Sutherland Brown, A., Brandon, M. T., Kanesewich, E. R., Hyndman, R. D. and Spencer, C., (1985). Lithoprobe, southern Vancouver Island: Seismic reflection sees through Wrangellia to the Juan de Fuca plate, *Geology*, **13**, 759-762.

Yuan, H., Park, J., and Levin, V., 1999. P-to-S converted phases from subducted slabs in the Northwest Pacific, *Eos trans. AGU*, **80**(46), Fall Meet. Suppl. F720.

Yuan, X., Sobolev, S. V., Kind, R., Oncken, O., Bock, G., Asch, G., Schurr, B., Graeber, F., Rudloff, A., Hanka, W., Wylegalla, K., Tibi, R., Haberland, Ch., Rietbrock, A., Giese, P., Wigger, P., Rower, P., Zandt, G., Beck, S., Wallace, T., Pardo, M., and Comte, D., (2000). Subduction and collision processes in the Central Andes constrained by converted seismic phases, *Nature*, **408**, 958-961.

Zelt, B. C., Ellis, R. M., and Clowes, R. M., (1993). Crustal velocity structure in the eastern Insular and southernmost Caost Belts, Canadian Cordillera, *Can. J. Earth Sci.*, **30**, 1014-1027.